Indian Journal of Pure & Applied Physics
Vol. 63, December 2025, pp. 1077-1087
DOI: 10.56042/ijpap.v63i12.14089

Vibrational Energy of Real Gas Molecules Impact on Calorimetric and Thermoelastic Coefficients

Brahim Ali Benyahia[a, c,*], Sidali Bensedira[b, c], Merouane Salhi[b, c] & Nardjes Bengherbia[b, c]

[a]Structure Laboratory, University of Blida, Blida 09 000, Algeria

[b]Energetic Process and Nanotechnologies Laboratory (LPEN), University of Blida, Blida 09 000, Algeria

[c]Department of Mechanical Engineering, Faculty of Technology, University of Blida, Blida 09 000, Algeria

Received:1st October 2024; accepted:24th September 2025

The aim of this work is to study the effect of gaseous imperfections of real gases on both calorimetric and thermo-elastic coefficients of gases. When we find that most of studies avoid going into this subject for the difficulty and complexity of its theory, especially on real gases, the latter is distinguished from the previous perfect gases due to the intermolecular interactions and presented by Berthelot state equation, which is more accurate than other equations of state. Here, A high-accuracy framework for predicting the calorimetric and thermoelastic properties of gases is introduced, after the development of new relationships based on the theory of real gases, a new general concept valid in any circumstance or condition, particularly at high pressure- temperature. Therefore, the effects of real gases leads to deviate from the behavior of perfect gases and, therefore, the coefficients based on this theory are different from those of perfect gases. Finally, an error given by the PG compared to the RG models for each coefficient is presented. The comparison is made for the purpose of determining an application limit of the PG model. The obtained results are very satisfactory and encouraging to deepen the advanced thermodynamics at high pressure.

Keywords: Calorimetric coefficients, Thermo-elastic coefficients, High temperatures-high pressures, Real gas model, Thermal- calorimetric imperfections

1 Introduction

Throughout history, scientists have played a role in expanding our knowledge of gases. How they behave. To illustrate during the 17th century Robert Boyle conducted experiments that shed light on the connection, between pressure and volume in gases setting the groundwork for what would later become known as the perfect gas law. Moving into the 19th century scientists formulated the theory of gases offering a microscopic perspective and understanding of the behavior of gases[1]. Calorimetric coefficients are used to quantify heat changes that occur during reactions or physical processes[2]. These coefficients provide information about the features of a system, such as heat capacity, enthalpy, and entropy[3,4]. Gas coefficients are vital for understanding the properties of these substances as well as optimizing industrial processes that use gases.The concept of coefficients goes back to the 18th century, when Antoine Lavoisier and Pierre Simon Laplace advocated employing calorimeters to monitor heat transfer during chemical reactions[5]. Julius Robert von Mayer established the concept of heat equivalents at the turn of the century, which led to advances in practical calorimeters[6]. As the century progressed, calorimetry became a technique in thermodynamics, physical chemistry, and materials science. The introduction of techniques such as scanning calorimetry and isothermal titration calorimetry made measuring calorimetric coefficients more exact and accurate[7]. Calorimetry still holds a position, in our comprehension of how energy's transferred and chemical reactions occur. We utilize coefficients to ascertain the heat capacities of gases and substances examine the thermodynamics of systems and create novel fluids or materials that possess enhanced thermal characteristics. Additionally, these coefficients enable us to investigate the behaviors of gases under temperatures and pressures which have implications, for various industrial and scientific applications[8]. Thermoelastic coefficients are measures that describe how temperature, pressure, stress, and strain affect the volume or density of fluids and materials[9]. Understanding how gases react in different contexts

*Corresponding author: E-mail: alibenyahia_brahim@univ-blida.dz

requires a solid grasp of these coefficients. This knowledge is applied in engineering and technology domains such as pressure vessel design, shock wave analysis, and gas dynamics in pipelines and storage tanks[10]. Thermoelastic coefficients have an important role in the development and design of high pressure and high temperature systems used in energy production and material processing[11]. It is critical to understand how gases react thermoelastically while building these systems. This understanding helps predict changes in volume and pressure, as well as optimize system efficiency to ensure safe processes involving these gases[12]. Many scientific studies, in this field often rely on the theory of perfect gas for its simplicity[13] including equations and their solutions. However, an issue arises when considering the calorimetric and thermo elastic coefficients of gases as they are influenced by some gas effects such as intermolecular interactions, imperfections behavior and compressibility effects[14]. Real gas effects cause deviations, from perfect gas behavior resulting in calorimetric coefficients compared to those of perfect gases[15]. Dealing with this matter can be a bit complex usually requiring methods to solve the equations that describe gas behavior under various thermodynamic conditions. The coefficients obtained through these methods can then be used to predict how gases behave in different scenarios[16]. With advancements, in the field of thermodynamics, in real gas thermodynamics researchers are continuously exploring the behavior of gases and developing new theories and models to gain a better understanding and predict their behavior under different conditions and for various applications. The field has seen some satisfactory and encouraging research papers on topics such as heat capacities[17,18], enthalpy[19], entropy[20], internal energy and work[21], free enthalpy and free energy[22] and various energetic issues related to gases[23-25]. These research efforts need completion, which primarily involves determining the calorimetric and thermo elastic coefficients, for advancing knowledge in thermodynamics.It is undeniable that we find some scattered works that deal with such field, but they are mostly not general, as some deal with specific phenomenon, as authers in reference[26-28], a specific gas[29,30], a specific coefficient[31-35], or use approximate methods[36-37], which makes the work lose its scientific value.While the thermo-elastic coefficients of gases have been neglected and the researcher's contribution is very small, as most of the references focus on solids or liquids[38-42]. To correct this imbalance, working on the computation of all calorimetric and thermo-elastic coefficients for real gas has become inevitable to move forward towards to advanced thermodynamics Computational thermodynamics, a field that combines engineering, physics and computer science employs computer simulations and numerical methods to analyze and make predictions, about the behavior of systems[43,44]. In this paper we take a approach using the Berthelot state equation. This empirical equation is known for its accuracy in describing the properties of gases compared to equations like the van der Waals equation or the Redlich Kwong equation[45]. One important advantage of the Berthelot state equation is that it explicitly considers forces, between gas molecules, which greatly influences the properties of gases[46,47]. This research paper has significant implications for a variety of sectors, including engineering, medicine, and the environment. The accompanying document provides background information on about 17 calorimetric and thermoelastic coefficients, as well as a brief discussion of the model and computing process employed. Results are provided for all coefficients at various pressures and temperatures. Using the Berthelot state equation, the developed relationships are fitted in the relevant temperature and pressure ranges of 150 K to 1000 K and 0.1 bar to 500 bar, respectively, to ensure adequate accuracy of the relationships for all regarded thermophysical properties.

2 Theoretical Review and Methodology

In a reversible transformation, the heat Q absorbed by a pure substance or a mixture of constant composition can be expressed using six calorimetric coefficients according to the variables followed during the transformation[48-49]:

$$\delta Q = C_v\ dT + l\ dV \quad \ldots (1)$$

$$\delta Q = C_p\ dT + h\ dP \quad \ldots (2)$$

$$\delta Q = \lambda\ dP + \mu\ dV \quad \ldots (3)$$

At constant pressure, relationships (2), and (3) become:

$$\delta Q = C_p\ dT \quad \ldots (4)$$

$$\delta Q = \mu\ dV \quad \ldots (5)$$

Putting equality between Eqs (1) and (4), we find the isothermal coefficient of expansion l which

represents the heat absorbed by during a variation of volume at constant temperature:

$$l = (C_p - C_v)\,(\frac{dT}{dV})_p \quad \ldots (6)$$

For the unnamed coefficient assigned to put Eq. (2) equal to Eq. (3), we find μ which represents the heat absorbed by the body during a change in volume at constant pressure:

$$\mu = C_p(\frac{dT}{dV})_p \quad \ldots (7)$$

At constant volume, then equations (1) and (3) can be written as follows:

$$\delta Q = C_v\ dT \quad \ldots (8)$$

$$\delta Q = \lambda\ dP \quad \ldots (9)$$

The isothermal compression coefficient *h* represents the heat absorbed during a pressure variation at constant temperature, and can be obtained by equality of Eq. (8) and (2) we find:

$$h = -(C_p - C_v).(\frac{dT}{dP})_V \quad \ldots (10)$$

The coefficient of linear expansion λ represents the heat absorbed by the body during a pressure variation at constant volume; λ is obtained by equality between Eq. (2) and Eq. (3) we find:

$$\lambda = C_v.(\frac{dT}{dP})_V \quad \ldots (11)$$

On the other hand, the Clapeyron formulas[44] present these coefficients in a different way:

$$l = T(\frac{dP}{dT})_V \quad \ldots (12)$$

$$h = -T(\frac{dV}{dT})_p \quad \ldots (13)$$

To formulate the relationships between the calorimetric and thermo-elastic coefficients, as well as to investigate the influence of pressure on a real gas (in this case, air), the Berthelot equation is used, which incorporates the effects of molecular size and intermolecular force. The Berthelot equation is written by[20]:

$$(P + \frac{a}{T\ V^2})(V - b) = R\ T \quad \ldots (14)$$

$$P(T,V) = \frac{R.\,T}{V - b} - \frac{a}{T.\,V^2} \quad \ldots (15)$$

where: $a = 3\ P_c V_c^{\,2} T_c$ and $b = \frac{V_c}{3}$

with P_c, V_c and T_c being the critical pressure, volume and temperature, respectively. Table 1 contains the critical parameters and properties of air.

The heat capacity at constant pressure Cp represents the heat absorbed during a variation in temperature at constant pressure; for a real gas this parameter is given by[17,24]:

$$C_p(T,\rho) = C_{P_{PG}}\left[1+\left(\frac{\gamma_{PG}-1}{\gamma_{PG}}\right)\left\{\frac{\left(\frac{\theta}{T}\right)^2\frac{Z}{(1-Z)^2}+}{\frac{2a\rho}{RT^2}\left[1+\frac{\left(\frac{2-b\rho}{1-b\rho}+\frac{a\rho}{2RT^2}\right)}{\frac{1}{(1-b\rho)^2}-\frac{2a\rho}{RT^2}}\right]}\right\}\right] \quad \ldots (16)$$

The heat capacity at constant volume C_V represents the heat absorbed during a temperature variation at constant volume; for real gases C_V is given by[23]:

$$C_V(T,\rho) = C_{v_{PG}}\left\{1+(\gamma_{gp}-1)\left(\left(\frac{\theta}{T}\right)^2\frac{e^{\left(\frac{\theta}{T}\right)}}{\left(1-e^{\left(\frac{\theta}{T}\right)}\right)^2}+\frac{2a\rho}{RT^2}\right)\right\} \quad \ldots (17)$$

The Laplace coefficient γ (ratio of specific heats) for the real gas is given by[18,21]:

$$\gamma(T,\rho) = \gamma_{(gp)}\left[\frac{1+\frac{\gamma_{(gp)}-1}{\gamma_{(gp)}}\left\{\left(\frac{\theta^2}{T}\right)\frac{\frac{\theta}{T}}{\left(1-e^{\frac{\theta}{T}}\right)}+\frac{4a\rho}{RT}\left[1+\frac{\left(\frac{2+b\rho}{1-b\rho}+\frac{a\rho}{2RT}\right)}{\frac{1}{(1-b\rho)^2}-\frac{2a\rho}{RT}}\right]\right\}}{1+(\gamma_{(gp)}-1)\left(\frac{\theta^2}{T}\right)\frac{\frac{\theta}{T}}{\left(1-e^{\frac{\theta}{T}}\right)^2}+\frac{2a\rho}{RT}}\right] \quad \ldots (18)$$

A new constant has been developed called C_T. Physically, C_T represents the heat absorbed during a volume variation at constant temperature[19]:

$$C_T(T,\rho) = \left(\frac{3\,a\,b^2\rho^3 - 6\,a\,b\,\rho - R\,T^3\,b + 3\,a}{2T\,\rho\,b - T\,b^2\rho^2 - T}\right) \quad \ldots (19)$$

Table 1 — Critical Parameters and Properties of Air[25]

Critical temperature Tc [K]	132.5
Critical pressure Pc [pas] * 10^6	37.7
Critical volume Vc [m^3] * 10^{-3}	3.22
Gas constant R [J/Kg. K]	287
Specific heats ratio γ	1.402
Constant of molecular vibrational energy θ [K]	3056
Specific heat capacity C_P [KJ/Kg. K]	1.004
Molar weight [g/mol]	28.97

The isobaric expansion coefficient or cubic expansion coefficient α, represents the relative change in volume due to a change in temperature at constant pressure, is given by[50]:

$$\alpha = \frac{1}{V}\left(\frac{\partial V}{\partial T}\right)_p \quad \ldots (20)$$

The isochoric compression coefficient or relative pressure coefficient β which is represents the relative pressure variation due to a temperature variation at constant volume; is given by[49]:

$$\beta = \frac{1}{P}\left(\frac{\partial P}{\partial T}\right)_V \quad \ldots (21)$$

By replacing this Eq. (20) in equation (13) and (21) in Eq. (12), we find:

$$l = T.P.\beta \quad \ldots (22)$$

$$h = -T.V.\alpha \quad \ldots (23)$$

Differentiate Eq. (15) at constant pressure:

$$dF = \left(\frac{\partial f}{\partial V}\right)_T dV + \left(\frac{\partial f}{\partial T}\right)_V dT \quad \ldots (24)$$

Substituting the partial derivatives in Eq. (24) we get:

$$dF = \left[\frac{-2a}{TV^3}(V-b) + \frac{RT}{(V-b)}\right]dV + \left[(V-b)\left(\frac{-a}{T^2V^2}\right) - R\right]dT \quad \ldots (25)$$

We can deduce:

$$\left(\frac{\partial V}{\partial T}\right)_P = \frac{a.V.(V-b) + T^2.V^3(V-b).R}{-2.a.(V-b)^2.T + R.T^3.V^3} \quad \ldots (26)$$

The isobaric expansion coefficient α, given by Eq. (20) became:

$$\alpha = \frac{(V-b)\left[a + R.T^2.V^2\right]}{R.T^3.V^3 - 2.a.T.(V-b)^2} \quad \ldots (27)$$

The isochoric compression coefficient β given by Eq. (21) became:

$$\beta = \frac{R.T^2.V^2 + a.(V-b)}{R.T^3.V^2 - a.T.(V-b)} \quad \ldots (28)$$

The isothermal compressibility coefficient which represents the relative change in volume due to a change in pressure at constant temperature, in this studyis given by[51]:

$$x_T = -\frac{1}{V}\left(\frac{\partial V}{\partial P}\right)_T \quad \ldots (29)$$

From[46], we have also:

$$x_T = \frac{\alpha}{\beta.P} \quad \ldots (30)$$

Substitute the Eq. (15), (27) and (28) in the Eq. (30) we obtain:

$$x_T = \frac{(V-b)\left[a + T^2.V^2\right]\left[T^2.V^2(V-b)\right]}{\left[R.T^3.V^3 - 2.a.T.(V-b)^2\right]\left[R.T^2.V^2 + a.(V-b)\right]} \quad \ldots (31)$$

The isothermal expansion coefficient *l* has been developed from Eq. (12) using Eq. (25), this latter became:

$$l = \left[\frac{R.T}{V-b} + \frac{a}{T.V^2}\right] \quad \ldots (32)$$

Similarly, Eq. (13) and (26) gives the isothermal compression coefficient h:

$$h = \frac{a.V.(V-b) + T^2.V^3.(V-b).R}{2.a.(V-b)^2 - R.T^2.V^3} \quad \ldots (33)$$

In thermodynamics, the relationship between the assigned unnamed coefficient μ, Cp and *h* is given by[39]:

$$\mu = -\frac{C_p.T}{h} \quad \ldots (34)$$

The linear expansion coefficient λ can be deduced by the following equation[40]:

$$\lambda = \frac{C_v.T}{l} \quad \ldots (35)$$

The isentropic compressibility coefficient is given by[52], it represents the relative variation of volume due to a variation of pressure at constant entropy:

$$x_s = -\frac{1}{V}\left(\frac{\partial V}{\partial P}\right)_Q \quad \ldots (36)$$

The relationship between the isentropic compressibility X_S, coefficient λ, and μ is given by[52]:

$$X_s = \frac{\lambda}{\mu.V} \quad \ldots (37)$$

The Thomson joule coefficient or Joule's second law is given by[53]:

$$\mu_{JT} = -\frac{1}{C_v}\left[T.\left(\frac{\partial P}{\partial T}\right)_V - P\right] \quad \ldots (38)$$

So, the Thomson joule coefficient becomes:

$$\mu_{JT} = -\frac{1}{C_v}\left[\frac{2.a}{T.V^2}\right] \quad \ldots (39)$$

The Isostatic modulus of elasticity or compression modulus K is the inverse of the isothermal coefficient of compressibility[12]:

$$K = -V(\frac{\partial P}{\partial V})_T \quad \ldots (40)$$

or:

$$K = \frac{1}{x_T} \quad \ldots (41)$$

The compressibility factor of a fluid, noted Z, is defined by[36]:

$$Z = \frac{PV}{RT} \quad \ldots (42)$$

The Joule-Gay-Lussac coefficient or Joule's first law has quantifies the change in temperature of a body as a function of its volume and given by[15]:

$$\mu_{JGL} = (\frac{\partial T}{\partial V})_U \quad \ldots (43)$$

The Grüneisen parameter is a dimensionless intensive quantity and given by[54]:

$$\tau = V(\frac{\partial P}{\partial U})_V \quad \ldots (44)$$

The relation between the coefficients and the thermodynamic potentials gives us easy ways to deduce some of the coefficients[9]:

The Coefficient of Joule-Gay-Lussac:

$$\mu_{JGL} = -\frac{(\beta.T - 1).P}{C_v} \quad \ldots (45)$$

The Coefficient of Joule-Thomson:

$$\mu_{GT} = \frac{(\alpha.T - 1).V}{C_p} \quad \mu_{GT} = \frac{(\alpha.T - 1).V}{C_p} \quad \ldots (46)$$

The Grüneisen Parameter:

$$\tau = \frac{\alpha.K}{\rho.C_v} = \frac{V.\alpha}{X_s.C_p} \quad \ldots (47)$$

In order to evaluate the coefficients derived from real gas theory RG, we will compare our model to other models. To do this, we offer the perfect gas model (PG), which depicts a thermal and caloric gas. This model is based on the perfect gas state equation, using specific heats CP, Cv, and their ratio γ as constants[5]. The calorimetric and thermo-elastic coefficients for the perfect gas model are shown in Table 2, below.

Table 2 — Calorimetric and Thermo-elastic Coefficients for the Perfect Gas Model [45, 48]

Heat capacity at constant volume C_V (J/Kg K)	γ/γ-1
Heat capacity at constant pressure C_P(J/Kg K)	γ R/γ-1
Laplace coefficient (ratio of specific heats) γ(//)	C_P/C_V
Unnamed coefficient assigned C_T (J/Kg K)	0
Isothermal coefficient of expansion *l* (Pa)	P
Isothermal compression coefficient *h* (m^3)	-V
unnamed coefficient assigned μ(Pa)	C_PT/V
linear expansion coefficient λ (m^3)	C_P T/P
Isobaric expansion coefficient α (K^{-1})	1/T
Isochoric compression coefficient β (K^{-1})	1/T
Isothermal coefficient of compressibility χ_T(Pa^{-1})	1/P
Isentropic compressibility coefficient X_S (Pa^{-1})	1/γP
Isostatic modulus of elasticity K (Pa)	P
Compressibility factor Z (//)	1
Joule-Gay-Lussac coefficient μ_{JGL}(K / m^3)	0
Grüneisenparameter Γ(//)	γ-1
Joule–Thomson coefficient μ_{JT}(K/Pa)	0

The majority of this work focuses on theoretical research, and we do a numerical calculation using the proposed calorimetric and thermo-elastic coefficients derived from real gas theory. We begin by applying the dichotomy approach[17] to identify the roots of the non-linear Berthelot state equation, which allows us to calculate the volume V at a given temperature T and pressure P. Unlike enthalpy[18], entropy[19], and internal energy[20], the equations for the derived coefficients are explicit and do not necessitate integration, derivation, or a complicated technique. We used FORTRAN power station for our calculation program since it is efficient and has high-speed computation capabilities[22].

3 Results and Discussion

In this section we will examine how the calorimetric and thermo elastic coefficients of a model representing real gases evolve. We will compare these evolutions with the results obtained from a model representing parfect gases. We aim to understand how temperature and pressure changes affect these coefficients and determine, under which conditions perfect gas behavior can be assumed. To present our findings we have developed a program that utilizes equations derived from the relationships between these coefficients in both models. This program allows us to visualize the changes in these coefficients and provide an explanation for any differences or contradictions, between the real gas model and the perfect gas model. By doing we can gain an understanding of how gases behave in reality.

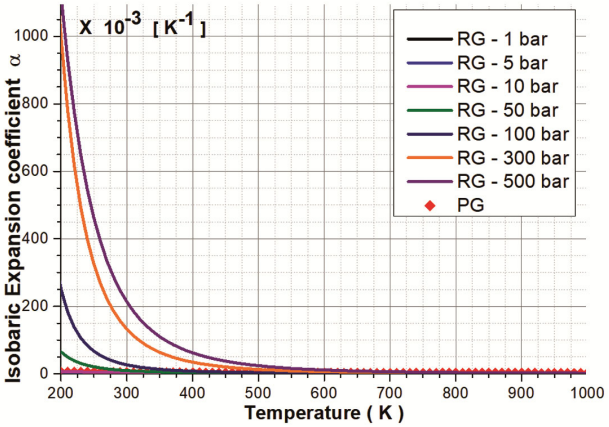

Fig. 1 — The isobaric expansion coefficient α variation versus temperature

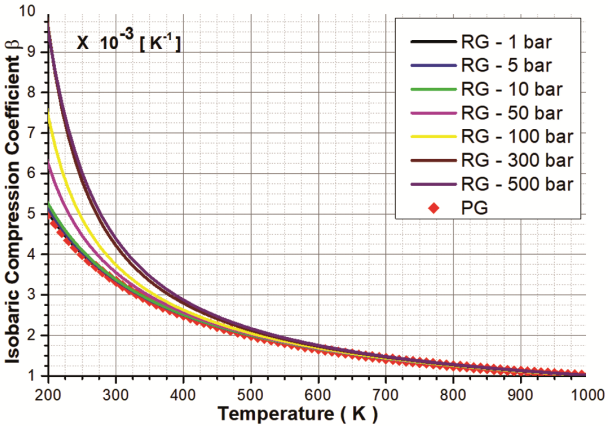

Fig. 2 — The isochoric compression coefficient β variation versus temperature

Figure 1 shows the variation of isobaric expansion coefficient α, with temperature at different pressure levels. We see that as the temperature T raises the isobaric expansion coefficient α decreases. At temperatures the results from the gas model differ from those of the ideal gas model but converge as the temperature increases. Moreover, increasing pressure leads to a value of α. For temperatures there is a deviation from the perfect gas model especially at high pressures (P = 500 bar) where differences can be up, to 1000 times. This variation highlights how pressure, temperature and gas imperfections impact α.

Figure 2 shows the variation of the isochoric compression coefficient, β, with temperature at different pressure levels comparing the Perfect Gas (PG) and Real Gas (RG) models. At temperatures both the RG and PG models follow a trend. However, as temperatures decrease a difference becomes apparent between the two models. The β value of the gas can potentially be that of the perfect gas at lower temperatures (e.g., at 500 bar). Beyond 700 K they

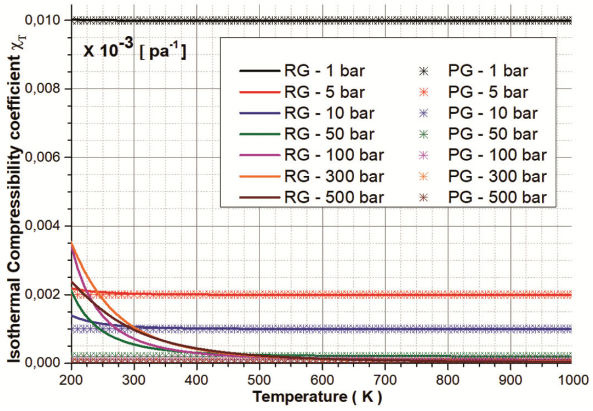

Fig. 3 — The isothermal compressibility coefficient χ_T variation versus temperature

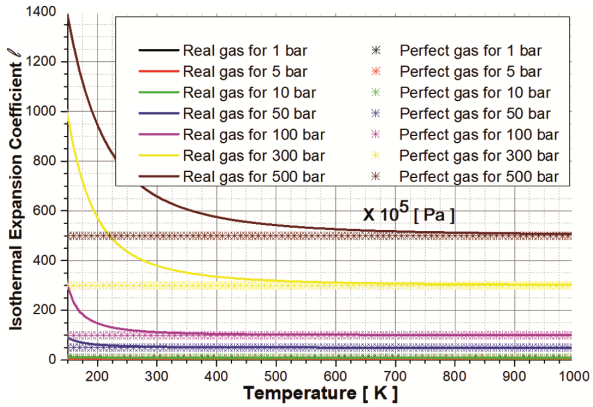

Fig. 4 — The isothermal expansion coefficient *l* variation versus temperature

come together. Demonstrate behavior, highlighting how pressure, temperature and gas imperfections impact β.

Figure 3 shows the isothermal compressibility coefficient, χ_T variation with temperature for different pressure levels. The graph indicates that the perfect gas curve remains a line suggesting that it only varies with pressure (χ_T = 1/P) and not temperature. In contrast the χ_T coefficient of real gases adjusts with both temperature (T) and pressure (P). As pressure increases the χ_T coefficient decreases, leading to a convergence of results between the two models. At temperatures both models follow a pattern; however, at lower temperatures there is a noticeable disparity between them. The χ_T coefficient of the real gas decreases until it aligns with that of the perfect gas model. For instance at T=300 K, the isothermal compressibility coefficient χ_T equals 5 10^{-8} and 10^{-6} pa^{-1} , for the perfect gas and real gas models respectively. This underlines how pressure temperature variations and gas imperfections impactχ_T.

Figure 4 depicts how the isothermal expansion coefficient, denoted as "*l* " changes, with temperature

at different pressure levels. The graph shows that the curve for a gas remains a line indicating that it stays constant with temperature but changes only with pressure (l = P). In contrast the l coefficient for real gases fluctuates with both temperature (T) and pressure (P). As pressure increases the l coefficient also rises, leading to a difference between the two models at lower temperatures. Eventually the l coefficient for gases decreases until it matches that of gases. At temperatures both models exhibit trends. For example at a pressure of 500 bar the isothermal expansion coefficient is 500 Pa for perfect gas and 660 10^5 Pa at 300 K and 545 10^5 Pa at 500 K for the real gas model. This discrepancy can be attributed to adjustments in pressure within the real gas equation of state highlighting how pressure temperature variations and imperfections, in gases influence the isothermal expansion coefficient "l."

Figure 5 depicts the variation of the isothermal compression coefficient h, with temperature for different pressure levels. One can see that higher pressure corresponds to a h value while increased temperature leads to a decrease in h. Moreover, it's noticeable that the perfect gas model yields trends (h = -V). Both models show patterns at temperature and pressure points up to P=10 bar. However, beyond this threshold distinctions, between the two models emerge. This difference diminishes as temperature and pressure rises.

Figure 6 shows the variation of the coefficient μ, with temperature across different pressure levels. It's clear that both higher pressure and temperature lead to an increase in the μ coefficient. The obtained results from the perfect gas model follows a line ($\mu = C_P T/V$). As temperature rises the two models start to diverge. Eventually come together. For instance at P=100 bar, μ_{PG} = 350 10^5 Pa and μ_{RG} = 185 10^5 Pa at T=500 K while they are 335 10^5 Pa, at T=800 K. We also notice that the degree of divergence decreases with increasing pressure. These results demonstrate how pressure, temperature and gas imperfections impact μ.

Figure 7 shows how the linear expansion coefficient, denoted as λ varies with temperature across different pressure levels encompassing both perfect gas and real gas models, from P=1 bar to 500 bar. As pressure rises λ decreases. Moreover, with increasing temperature the models display discrepancies though these differences lessen at higher pressures. This finding highlights the impact of pressure temperature fluctuations and gas imperfections, on λ.

Figure 8 shows the variation of the isentropic compressibility coefficient, X_S with temperature at different pressure levels. A key observation is that higher pressure leads to a decrease in a X_S value.

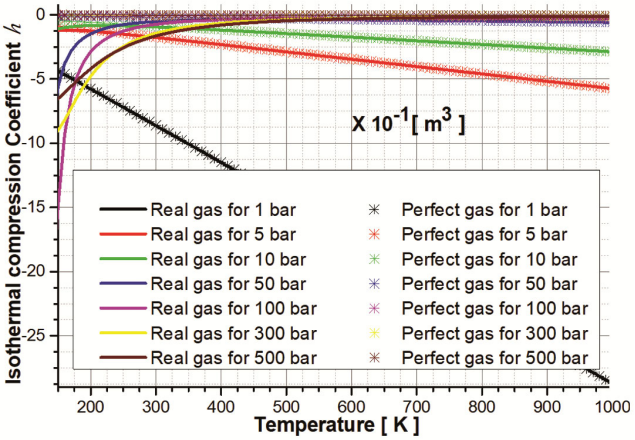

Fig. 5 — The isothermal compression coefficient h variation versus temperature

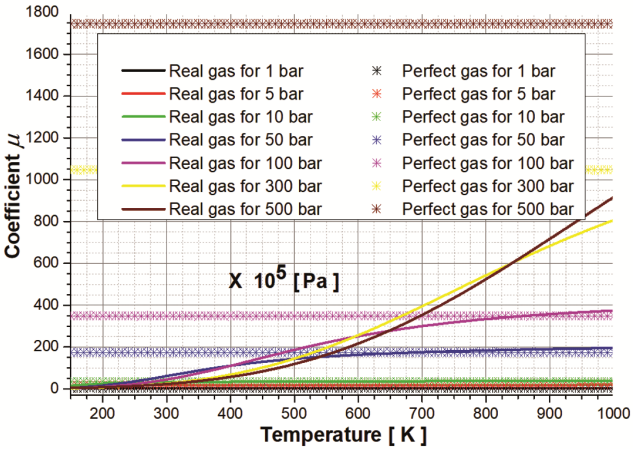

Fig. 6 — Variation of μ coefficient versus temperature

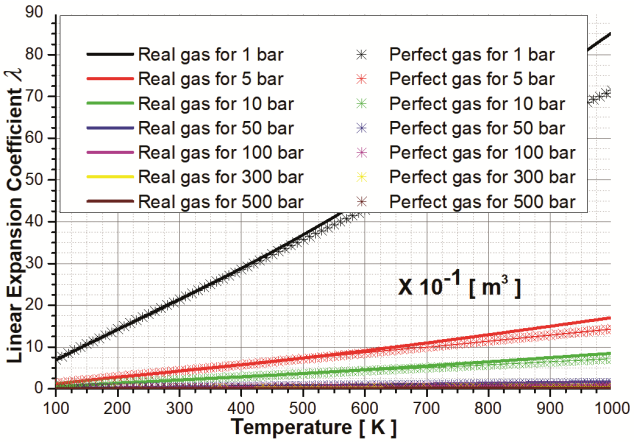

Fig. 7 — The linear expansion coefficient λ variation versus temperature

Moreover, the graph representing the perfect gas model a horizontal line (X_S = 1/γP) while there is a divergence between the two models at certain (low) temperatures highlighting the impact of imperfections, on this coefficient. Otherwise, the variation of the isostatic modulus of elasticity, K, as a function of temperature for several pressure values, which is shown in the fig. 9. Here we can note that, the increases in both pressure and temperature results in an increase in the K coefficient. Additionally, at specific temperatures, the results obtained from the perfect gas model form horizontal straight lines (K = P), but at other temperatures, the two models diverge, gradually approaching each other as temperature increases. For instance, at P=100 bar, K_{PG}= 100 10^5 Pa, K= 73 10^5 Pa and 92 10^5 for T=600 K and 900 K, respectively. This highlights the effects of pressure, temperature, and gas imperfections on K.

Figure 10 represents the variation of the Joule Gay Lussac coefficient, μ_{JGL}, with temperature, for several pressure values. It's clear that as temperature rises the Joule Gay Lussac coefficient increases, while it decreases with pressure. Interestingly a perfect gas always has a μ_{JGL} value of zero ($\mu_{JGL\text{-}GP}$=0). The curves gradually approach zero as temperature increases. The increase rate varies based on the pressure applied. Higher pressures give a significant value of μ_{JGL}at low temperature and leads to a quickly decrease towards zero. For instance, at a temperature of T=400 K, μ_{JGL} is approximately -8.14 10^{-5}, -0.002, -0.008, -0.191, -0.7146, -4.893 and -10.445 K / m^3 for pressures of 1, 5, 10, 50, 100, 300, and 500 bar, respectively. In contrast to Fig. 10 is Fig. 11 which represents the variation of the Joule-Thomson coefficient, μ_{JT}, as a function of temperature for several pressure values. In this case the Joule Thomson coefficient increases with increasing pressure and decreases with increasing temperature, for example, at a temperature T=400 K, μ_{JT} is approximately 0.05 10^{-5}, 0.18 10^{-5}, 1.29 10^{-5},

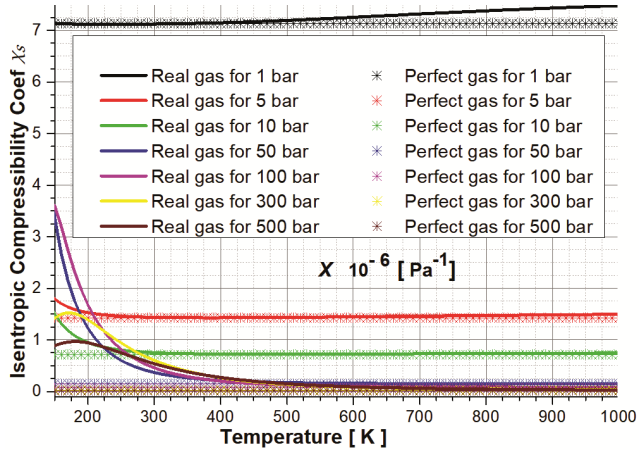

Fig. 8 — The isentropic compressibility coefficient X_S variation versus temperature

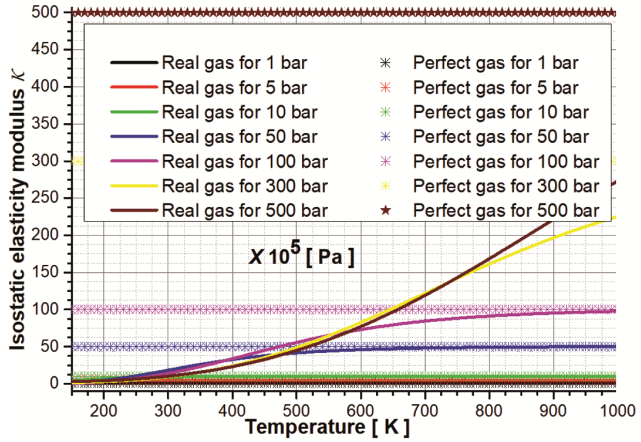

Fig. 9 — The Isostatic modulus of elasticity K variation versus temperature

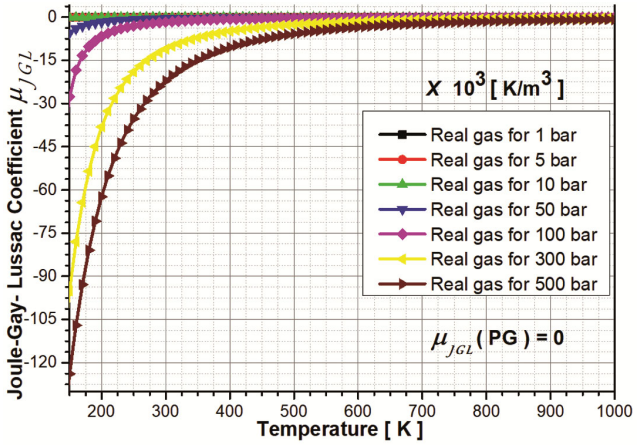

Fig. 10 — The Joule-Gay-Lussac coefficient μ_{JGL} variation versus temperature

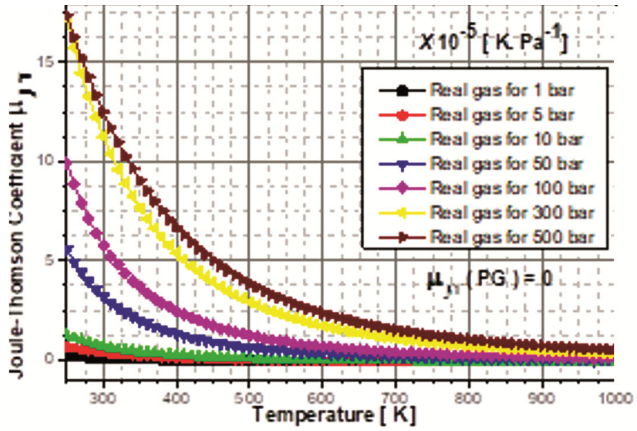

Fig. 11 — The Joule-Thomson coefficient μ_{JT} variation versus temperature

2.45 10^{-5}, 5.46 10^{-5} and 6.5 10^{-5}K/Pa for pressures of 5, 10, 50, 100, 300, and 500 bar, respectively. This illustrates how pressure, temperature and gas imperfections impact μ_{JGL} and μ_{JT}.

Figure 12 shows the Grüneisen parameter Γ variation, with temperature at different pressure levels. It is clear that as pressure increases the Grüneisen coefficient also increases, while it decreases with rising temperature. Notably the value of Γ remains constant for the perfect gas (Γ = γ - 1). For instance, at a temperature of 400 K the values of Γ are approximately 397.34 10^{-3}, 399.21 10^{-3}, 401.5610^{-3}, 420.43 10^{-3}, 444.07 10^{-3}, 538.05 and 629.65 10^{-3} for pressures of 1, 5, 10, 50, 100, 300, and 500 bar, respectively. The perfect gas has a Γ value of around ~0.408, this results prove how pressure, temperature and gas imperfections can impact this parameter.

Figure 13 illustrates the variation of the compressibility factor Z with temperature at different pressure levels. The compressibility factor Z for perfect gas model Z stays constant at Z = 1. However, in the real gas model Z is affected by changes, in both pressure and temperature. In conditions with standard pressure and temperatures we can estimate that Z behaves like a perfect gas. However, with a change in pressure the compressibility factor for air deviates from 1 especially at low temperatures due to intermolecular forces and molecular interactions. However, it returns to align with the perfect gas at high pressures and temperatures. The compressibility factor is calculated using the Berthelot equation of state. The graph demonstrates that as pressure rises Z also increases. At a pressure of 500 bar under low temperature conditions it can be up to 2.5 times higher. As temperature increases Z decreases and curves for pressures get closer, within the range of 1.0 to 1.2 starting at 800 K.

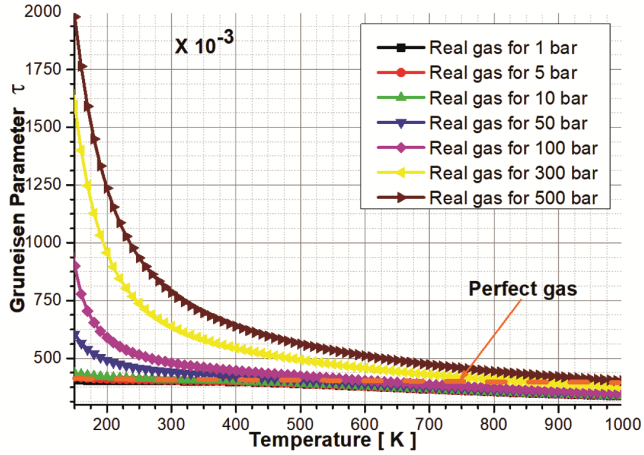

Fig. 12 — The Grüneisen parameter Γ variation versus temperature

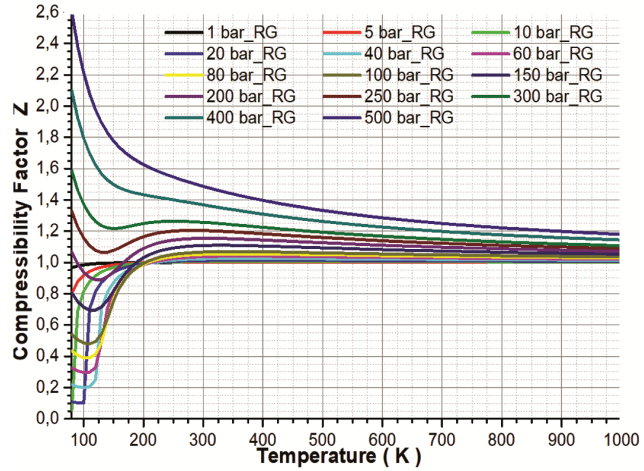

Fig. 13 — The Compressibility Factor Z variation versus temperature

4 Conclusion

The determination of calorimetric and thermoelastic coefficients in thermodynamics is crucial for understanding and predicting the behavior of gases under various thermal and mechanical conditions. The developed model of these coefficients for real gases was investigated in this paper. Knowing that, most studies avoid tackling this subject because of the difficulty and complexity of its theory, particularly on real gases. This study is divided into two parts. First, we treated the coefficients applicable to perfect gases. Second, we studied the coefficients for real gases. Finally, a comparison was made between the two models. Understanding and the computation of the thermoelastic and calorimetric coefficients, in thermodynamics is crucial for gaining insights into gases and thermal systems. This knowledge plays a role in developing solutions, for present and future technological hurdles as well as enhancing the energy efficiency and longevity of energetic systems. The results show, that the pressure, the temperature, the caloric and thermal imperfections have an impact on the behavior of both real and perfect gases. The calorimetric and the thermoelastic coefficients differ between perfect and real gases at low temperatures and high pressures for α, β, *l*, *μ*, *K*, Γ and Z. At low temperatures and pressures for $\chi_T$and *h*. At high temperatures and low pressures for λ. At high temperatures and pressures for X_S. As for $\mu_{JGL}$and μ_{JT}, their value is equal to zero for the perfect gas model. Therefore, they differ from the real gas under all conditions. Which leads to asymmetric behavior. However, when the conditions are reversed,

the behavior of real gases is similar to that of perfect gases, and their coefficients become identical. In all cases, it is observed that when the temperature is below 500K or at high pressure, we strongly recommend using real gas laws. Moreover, without a thorough comprehensive understanding of gas thermodynamics, it is impossible to calculate calorimetric and thermoelastic coefficients. Alternative substances can be chosen instead of air, and the relationships will still apply. It is necessary to determine the molecular force constants and molecular size, as well as the temperature of the characteristic vibrations. The relationships of perfect gas can be simplified by removing constants related to molecular forces (a), molecular size (b) and the vibrational characteristic temperature (Θ), from the real gas model. This simplification transforms the real gas model into a case of our model which is the PG model. When the conditions referred to in the previous paragraph are reversed, we find a difference between the outcomes of the perfect gas model (PG) and the real gas model (RG) in terms of certain calorimetric and thermoelastic coefficients with increases of deviations. Hence it is necessary to apply the real gas relationships for analyzing the behavior of gases. The new relationships are useful across scenarios and conditions of pressures and temperatures, On the other hand, the use of PG model reveals significant discrepancies underscoring the importance of employing the RG model for more accurate results. The calorimetric and thermoelastic coefficients can be expressed as second partial derivatives of the thermodynamic potentials internal energy U, enthalpy H, free energy F and free enthalpy G with respect to their natural variables volume V, entropy S, pressure P and temperature T respectively. These coefficients are related to thermodynamic potentials, and their signal has a strong and direct impact on thermodynamic stability. Under five stability conditions, thermodynamic references are used to translate them into calorimetric and thermoelastic coefficients: 1- $C_P \geq C_V \geq 0$, 2- $x_T \geq 0$, 3- $x_S \geq 0$, 4- $\lambda^2 \geq T\, C_V\, V\, x_S$ and 5- $C_P\, x_T \geq T V\, \alpha^2$. It is therefore possible, if we can measure two of the three thermoelastic coefficients (α, β and χ_T), to establish an equation of state. Where that if only α and β are known, it possible to determine χ_T, otherwise, the knowledge of α can be replaced by that of h, β by l and χ_T by K.

References

1 Müller I, A History of Thermodynamics: The Doctrine of Energy and Entropy (Springer Berlin), 1st Edn, 2007, p. 9.
2 MacLeod B P, Schauer P A, Hu K Lam B, Fork D K & Berlinguette C P, *Rev SciInstrum*, 88 (2017) 084101.
3 Ghosh M K, Elliott S N, Somers K P, Klippenstein S J & Curran H J, *Combust Flame*, 257 (2023) 112491.
4 Tahir-Kheli R, General and Statistical Thermodynamics (Springer, Cham), 1st Edn, 2020, p. 265.
5 Truesdell CA, TheTragicomical History of Thermodynamics (Springer, New York), 1st Edn, 2013, p. 29.
6 Helm G, The Historical Development of Energetics (Springer, Dordrecht), 1st Edn, 2000, p. 181.
7 Davies S R, Lachance J W, Sloan E D & Koh C A, *Ind Eng Chem Res*, 49 (2010) 12319.
8 Wilhelm H, 'AC-calorimetry at high pressure and low temperature' in *Advances in Solid State Physics*, edited by B Kramer (Springer, Berlin), 2003, p. 889.
9 Cornu A, *J Phys Theor Appl*, 2 (1873) 41.
10 Das M, Liu S H & Tsai Y T, *Thermochim Acta*, 656 (2017) 90.
11 Navrotsky A, *Phys Chem Miner*, 2 (1977) 89.
12 Toual Y, Mouchou S, Azouaoui A, Maouhoubi A, Hourmatallah A, Benzakour N & Bouslykhane K, in *Chem Phys,* 572 (2023) 111967.
13 Bonnefoy O, Thermodynamique (École Nationale Supérieure des Mines, Saint-Étienne), 1st Edn, 2016, p. 15.
14 Weiss S, Polansky J, Bar M, Oberleithner K & Schmelter S, *Int J Hydrogen Energy*, 48 (2023) 23456.
15 Pakravesh A & Zarei H, *Cryogenics*, 118 (2021) 103350.
16 Kolesnikov I M, *Chem Pet Eng*, 35 (1999) 35.
17 Salhi M, Zebbiche T & Mehalem A, *Proc Inst Mech Eng G J Aerosp Eng*, 231 (2017) 326.
18 Salhi M, Bensedira S & Bennoud S*, J Inst Eng India Ser C*, 105 (2024) 1047.
19 Salhi M & Roudane M, *High Temp High Press*, 48 (2019) 321.
20 Salhi M, Ketfi O & Roudane M, *Rom J Phys*, 68 (2023) 609.
21 Salhi M & Zebbiche T, *Thermal effects in high-speed aerodynamics*, paper presented at the 8th AIAA Theoretical Fluid Mechanics Conference, Denver, USA, 5-9 June 2017.
22 Salhi M, Bensedira S & Bengherbia N, *Indian J Phys*, 98 (2024) 4849.
23 Salhi M, *Improvement of supersonic nozzles performances by a new design method*, paper presented at the AIAA Aviation 2023 Forum, San Diego, USA, 12-16 June 2023.
24 Li C, Jia W & Wu X, *Energy Procedia*, 14 (2012) 115.
25 Bengherbia N Salhi M & Roudane M, *Indian J Phys*, 98 (2024) 2461.
26 Chamkalani A, Zendehboudi S,Chamkalani R,Lohi A, El Kamil A & Chatzis I, *Fluid Phase Equilib*, 358 (2013) 189.
27 Volejníková B, Hovorka Š, Řehák K & Bartovská L, *Fluid Phase Equilib*, 283 (2009) 65.
28 Li J Q, Chen Y, Ma Y, Kwon J T, Xu H & Li J C, *Case Stud Therm Eng*, 41 (2022) 102678.
29 Kamari A, Gharagheizi F, Mohammadi A H & Ramjugernath D, *J MolLiq*, 216 (2016) 25.
30 Li Z, Zhang C, Li C, Wu X,Xie H & Jiang L, *J Clean Prod*, 406 (2023) 137074.

31 Ernst G, Keil B,Wirbser H & Jaeschke M, *J Chem Thermodyn*, 33 (2001) 601.
32 Voëadlo N & Price G D, *Phys Earth Planet Inter*, 82 (1994) 261.
33 Peng Z, Xie W, Meng S, Han X, Wang H & Du S, *Measurement*, 159 (2020) 107766.
34 Su G, Chen L & Chen J, *Phys Lett A*, 378 (2014) 1992.
35 Hafsi Z, Elaoud S A, Akrout M & Tahar S, 'New correlation for hydrogen-natural gas mixture compressibility factor' in *Design and Modeling of Mechanical Systems-II*, edited by L Walha *et al*. (Springer, Cham), 2015, p. 791.
36 Dehli M, Doering E & Schedwill H, Fundamentals of Technical Thermodynamics (Springer, Wiesbaden), 1st Edn, 2022, p. 151.
37 Chatterjee S & Chattopadhyay S, *Superlattices Microstruct*, 101 (2017) 384.
38 Egorov G I, Makarov D M & Kolker A M, *Fluid Phase Equilib*, 354 (2013) 133.
39 Das D K, Bhattacharjee H, Sahoo S K & Sahoo N, *Mater Today Proc*, (2023), in press.
40 Irvine T F Jr & Duignan M R, *IntCommun Heat Mass*, 12 (1985) 465.
41 Ricken T & de Boer R, *Solid Mech Appl*, 125 (2005) 359.
42 Liu Z K, *Acta Mater*, 200 (2020) 745.
Lukas H L, Fries S G & Sundman B, Computational Thermodynamics: The Calphad Method (Cambridge University Press, Cambridge), 1st Edn, 2007, p. 203.
43 Ruggeri T, Sugiyama M, Classical and Relativistic Rational Extended Thermodynamics of Gases (Springer, Cham), 1st Edn, 2021, p. 219.
44 Struchtrup H, Thermodynamics and Energy Conversion (Springer, Heidelberg), 1st Edn, 2014, p. 289.
45 Boulos M I, Fauchais P L & Pfender E, Handbook of Thermal Plasmas (Springer, Cham), 1st Edn, 2023, p. 103.
46 Hentschke R, Thermodynamics (Springer, Cham), 2nd Edn, 2022, p. 261.
47 Foust H C III, Thermodynamics, Gas Dynamics, and Combustion (Springer, Cham), 1st Edn, 2022, p. 25.
48 Bernal P J & Van Hook W A, *J Chem Thermodyn*, 18 (1986) 969.
49 Bellos E,Vrachopoulos M G &Tzivanidis C, *Therm Sci Eng Prog*, 11 (2019) 239.
50 Yaws C L, Thermophysical Properties of Chemicals and Hydrocarbons (Gulf Professional Publishing, Oxford), 2nd Edn, 2014, p. 499.
51 Kumar A, Sharma S, Singh K & Yadav S, *J Chem Thermodyn*, 150 (2020) 106228.
52 Pistun E P, Matiko F D & Masnyak O Y, *Meas Tech*, 52 (2009) 509.
53 Borissenok V A, *Russ Phys J*, 58 (2015) 249.